

LOSS’S First Supernova: New Limits on the “Impostor” SN 1997bs

Scott M. Adams¹ & C.S. Kochanek^{1,2}

¹ Dept. of Astronomy, The Ohio State University, 140 W. 18th Ave., Columbus, OH 43210

² Center for Cosmology and AstroParticle Physics (CCAPP), The Ohio State University, 191 W. Woodruff Ave., Columbus, OH 43210

E-mail: sadams@astronomy.ohio-state.edu

19 June 2022

ABSTRACT

We present new, late-time *Hubble Space Telescope* and *Spitzer Space Telescope* observations of the archetypal SN impostor SN 1997bs. We show that SN 1997bs remains much fainter than its progenitor, ruling out the canonical picture of late-time obscuration by dust forming in a shell ejected during the transient. The possibility that the star survived cloaked behind a dusty, steady wind is also disfavored. The simplest explanation is that SN 1997bs was a subluminous Type IIn SN, although it is impossible to rule out the possibility that the star survived, but with a significantly decreased intrinsic luminosity.

Key words: stars: evolution – supergiants – supernovae: general – supernovae: individual (SN 1997bs)

1 INTRODUCTION

Supernova (SN) impostors (Van Dyk et al. 2000) are a class of stellar transients characterized by Type IIn spectra (narrow hydrogen emission lines) with lower peak luminosities ($M_V \simeq -13$) than typical core collapse SNe (ccSNe; $M_V \simeq -17$). The class is heterogeneous, including luminous variable stars (e.g. SN 2002kg; Weis & Bomans 2005) and the SN 2008S class of transients (Prieto et al. 2008; Thompson et al. 2009; Kochanek 2011a), but a subset of the events are generally connected to some type of eruptive transient associated with the phenomenology of Luminous Blue Variable stars (LBV; Humphreys & Davidson 1994). Still, the true nature of SN impostors is debated, including whether they are non-terminal eruptions or actual SNe (see Smith et al. 2011; Kochanek et al. 2012).

The rate of SN impostors attributed to LBV eruptions is likely $\sim 20\%$ – 60% of the ccSN rate (Thompson et al. 2009). Thus, the true nature of these transients could have important consequences for the rate of SNe. For example, the SN rate appears to be less than the massive-star formation rate (Horiuchi et al. 2011). There are several possible solutions to this mismatch. Non-local SN surveys could be significantly incomplete (e.g., Botticella et al. 2012) or there could be a significant rate of failed SNe (Kochanek et al. 2008; Gerke et al. 2014). The latter solution could also help to explain the lack of higher mass SN progenitors ($\gtrsim 15 M_\odot$; Kochanek et al. 2008; Smartt 2009) and the black hole mass function (Kochanek 2014a,d). The final option is that some of these

lower luminosity transients are in fact SNe (Horiuchi et al. 2011).

On the other hand, if SN impostors are non-terminal events, they may be the dominant mode of mass loss in massive stars (Smith & Owocki 2006). This would be important because eruptive mass loss is unaccounted for in stellar evolution models and little is known about the mechanism, duty cycle, mass dependence, or total mass loss in such events. Recently Khan et al. (2013, 2014) surveyed nearby galaxies and found that luminous stars encased in ejected dusty shells analogous to η Carinae are not common enough for eruptions to be the dominant mass loss channel, representing $\sim 10\%$ of mass loss rather than $\sim 50\%$.

Inspired by the phenomenology of η Carinae, the most-widely accepted picture of SN impostors is that these events are the result of non-terminal eruptions that eject a significant amount of mass that then may obscure the surviving star (see e.g., Humphreys et al. 1999). The phenomenology expected for a dusty shell is fairly simple – the optical depth peaks as the shell passes through the dust formation radius and then declines as $\sim t^{-2}$ with time (Kochanek 2011b). Kochanek et al. (2012) examined several SN impostors with archival *HST*, *SST*, and *Large Binocular Telescope* (LBT) data and found that none of the transients (for which there is sufficient data to reach a conclusion) are consistent with the shell ejection scenario. If they are simply outbursts, the data are more consistent with a scenario where the transient is a sign post that the star is transitioning from a low to a high mass-loss rate, resulting in a longer lived dusty wind.

Still, nothing in the available data ruled out the possibility that some of these systems are not impostors at all, but instead are true SNe.

The basic problem is that SN impostors have been little studied after the brief optical transient even though it is really the late-time phenomenology that is the key to understanding these events. For example, it would be useful to simply establish the continued presence of a star. In this paper we utilize new late-time observations to investigate the nature of the archetypal impostor SN 1997bs.

SN 1997bs, discovered on 1997 April 15, was the first SN reported by the Lick Observatory Supernova Search (LOSS; Treffers et al. 1997). It was found in NGC 3627 and was classified as a Type II_n supernova (the spectrum was dominated by Balmer emission lines with FWHM $\simeq 1000$ km/s). Van Dyk et al. (1999) identified a candidate progenitor with $m_{F606W} \simeq 22.86 \pm 0.16$ mag, which corresponds to a luminosity of $L_* = 10^{4.8}-10^{5.4} L_\odot$ for the temperature range $T_* = 7500-20,000$ K. The event peaked at $V \simeq 17$ and had faded to (F555W) $V \simeq 23.4$ mag by 10 January 1998. Over this period the transient became redder, evolving from $V - I = 0.7$ to $V - I = 3$ mag (Van Dyk et al. 2000). Van Dyk et al. (2000) suggested that the flattening of the late-time light curve at ~ 0.5 mag fainter than the progenitor was an indication that the star survived the explosion.

In fact, it continued to fade, since Li et al. (2002) found that the SN was marginally detected in an *HST*/WFPC2 image taken in 2001, with F555W = 25.8 ± 0.3 mag (March 4) and that it was not detected at F814W to a limiting magnitude of about 25.0 (February 24 and May 28). Li et al. (2002) posited that while the formation of dust in the ejecta could explain the continuous decline in the optical flux, this would be inconsistent with the color evolution. The SN would become progressively redder if dust was forming in the ejecta, but instead the source appeared to become bluer between early 1998 and early 2001. We present the full optical light curve in Fig. 1.

Van Dyk & Matheson (2012) reported mid-infrared emission near the position of SN 1997bs in *Spitzer* IRAC images from 2004 May, with 32 μ Jy at 3.6 μ m and 40 μ Jy at 4.5 μ m, but no detections at 5.8 μ m and 8.0 μ m. Van Dyk & Matheson (2012) stated that this could be fit by a $T \simeq 970$ K blackbody with a radius $R \simeq 1.4 \times 10^{15}$ cm and luminosity $L \simeq 3.1 \times 10^5 L_\odot$. This would correspond to an expansion speed of only ~ 60 km/s, far slower than the ~ 765 km/s line width observed during the transient (Smith et al. 2011). Additionally, Van Dyk & Matheson (2012) found that the star is recovered at $m_{F555W} = 26.08$ and $m_{F814W} = 25.08$ mag in *HST*/ACS data obtained in 2009, although they do not report uncertainties.

Kochanek et al. (2012) considered the same *Spitzer* observations but had a different interpretation. Kochanek et al. (2012) found that most of the flux of the point source possibly present in the 4.5 μ m image vanished in wavelength-differenced images¹, suggesting that the source of the flux

¹ Using difference imaging methods to subtract the 3.6 and 4.5 μ m images removes all sources with the “Rayleigh-Jeans” mid-IR spectral energy distributions of normal stars to leave only those with significant dust emission. Thus, the lack of a counterpart in the wavelength-differenced images indicates an absence of dust emission.

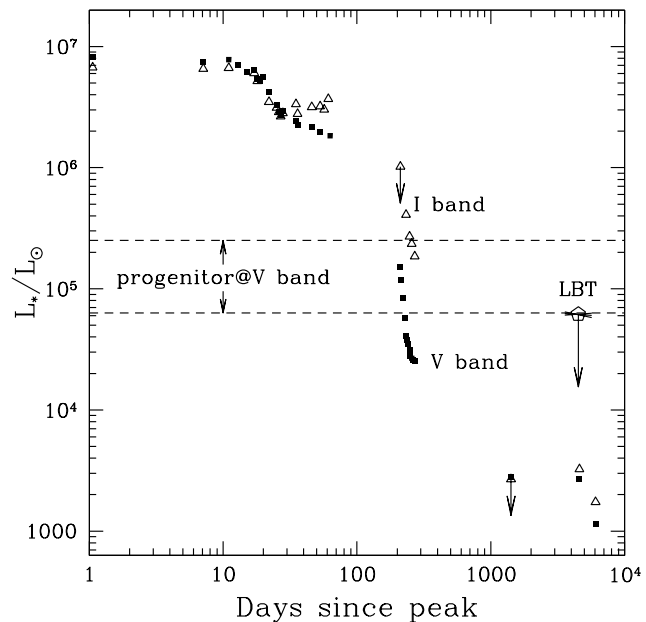


Figure 1. Optical light curve of SN 1997bs. The filled squares (open triangles) show the evolution of the V-band (I-band) luminosity. The last set of V and I-band luminosities represent the upper limits we find for the new *HST* data we present in this paper. The short lines extending from the *LBT* point (the open pentagon) represent the V-band variability and 3σ limits found by image subtraction of our *LBT* monitoring data. The horizontal dashed lines give the range of progenitor luminosities for $T_* = 7500 - 20,000$ K given the candidate progenitor detection of $m_{F606W} \simeq 22.86 \pm 0.16$ mag reported by Van Dyk et al. (1999).

was not dusty. Furthermore, Kochanek et al. (2012) found that the evolution of the spectral energy distribution (SED) is inconsistent with the ejection of a single shell at the time of the transient. Keeping the star obscured at the time of the *HST* observations in 2001 would require a continued mass-loss rate of $\dot{M} \sim 10^{-3} M_\odot \text{yr}^{-1}$. However, matching the candidate surviving star to the progenitor requires a temperature ($T_* > 10^4$ K), too high to allow the formation of dust (see Kochanek 2011a, 2014c). Kochanek et al. (2012) concludes that if the star found by Li et al. (2002) is the survivor of SN 1997bs, the most likely scenario is that the eruption ended before 2001 and the star would have to be unobscured in 2011.

In this work we revisit these questions with new *HST*, *Spitzer*, and *LBT* observations. In §2 we present the data, explain our identification of the source and its photometry, and present the methods we use to model and constrain the existence of a surviving star. As can be seen from Fig. 2, no star is obviously visible, and there is certainly no source with a flux comparable to the progenitor. In §3 we present the results of modeling the SED of the source as obscured by an expanding shell or a steady-state wind and show that they are inconsistent with a surviving star as luminous as the progenitor. Finally in §4 we summarize our results and consider alternative explanations for the fate of SN 1997bs. When converting observables into physical quantities we adopt the Cepheid distance of 9.4 Mpc to NGC 3627 from Freedman et al. (2001) and a Galactic extinction

of $E(B - V) = 0.04$ from the Schlafly & Finkbeiner (2011) recalibration of Schlegel et al. (1998). We note that this results in a significantly smaller progenitor luminosity than that adopted by Van Dyk et al. (2000), who used an older Cepheid distance of 11.1 Mpc from Saha et al. (1999) and also included an estimate of galactic reddening from NGC 3627 of $E(B - V) = 0.21$ mag. Though we do not include this galactic reddening, such reddening, to first order, will be taken into account by our circumstellar dust models (but see Kochanek et al. 2012). Additionally, most of our results are dependent primarily on the luminosity of the progenitor relative to a possible survivor, which is independent of foreground extinction and the adopted distance.

2 DATA AND MODELS

2.1 Data

We utilize both new and archival *HST* data. For our program we obtained new WFC3 UVIS F555W and F814W and IR F110W and F160W images (GO-13477) taken in November 2013. We also use public *HST* WFC3 UVIS F275W, F336W, F438W, F555W, and F814W images taken for the Legacy ExtraGalactic UV Survey (LEGUS; PI D. Calzetti, GO-13364) in February 2014 and the multi-epoch archival WFC2 F555W images of NGC 3627 taken between late 1997 and early 1998 (PI A. Sandage, GO-6549) that contain the transient event to calibrate our astrometry and measure the position of SN 1997bs. Additionally we analyze archival ACS/WCS F555W and F814W images taken in December 2009 (PI S. van Dyk, GO-11575) and F435W images taken in December 2004 (PI R. Chandar, GO-10402).

We make use of new and archival *Spitzer* data. We coadded archival images of NGC 3627 (from program ID 159) taken in May 2004 and also coadded archival images taken in Feb-March-Aug 2014 (ID 10136) together with data from our program (ID 10001) taken in July 2013 using the MOPEX reduction package². We also performed image subtraction of these data using ISIS (Alard & Lupton 1998; Alard 2000) to check for source variability.

We have been monitoring NGC 3627 with the *LBT* as part of a program searching for failed SNe (Kochanek et al. 2008; Gerke et al. 2014). We use ISIS to check for optical source variability in the dozen epochs we have collected between 2008 and 2014.

2.2 Candidate Identification

Proper alignment of all the data and a precise measurement of the coordinates of SN 1997bs are critical for correct candidate identification and photometry. We first aligned and stacked the archival drizzled *HST* WFC2 F555W images using SEXTRACTOR (Bertin & Arnouts 1996), SCAMP (Bertin 2006), and SWARP (Bertin et al. 2002). We chose to register the astrometry of all our data to the drizzled *HST* WFC3 F814W image from November 2013. We found the position of SN 1997bs in our reference WFC3 F814W frame by aligning the stacked archival WFC2 F555 image

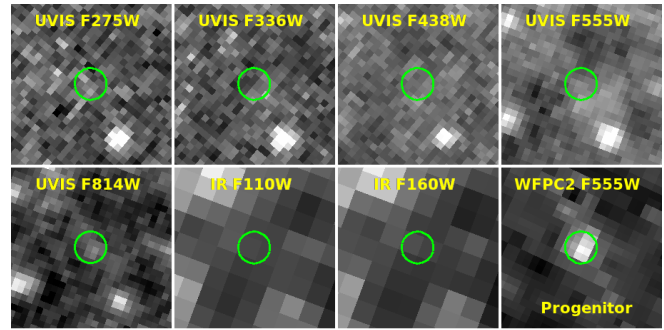


Figure 2. The region surrounding SN 1997bs in the new *HST* WFC3 images and the pre-SN WFC2 F555W image. The radius of the green circles ($0''.1$) is 25 times our positional uncertainty and each image is $1''.0$ across.

with the GEOMAP task in IRAF³ using a matched coordinate list of several dozen sources within $20''$ of SN 1997bs. We estimate an uncertainty of $0''.002$ in the astrometry by measuring the RMS in the SN position using different subsamples of the matched coordinate list with different orders for the astrometric fits. We measure a centroid uncertainty of $0''.004$ based on the aperture photometry of SN 1997bs in the stacked archival frame. Adding these uncertainties in quadrature gives a total positional uncertainty of $0''.004$ (0.1 pixels) in our reference image.

We generate photometric catalogs for the *HST* WFC3 data using the software package DOLPHOT 2.0 (Dolphin 2000)⁴. We largely used the same parameter settings as Dalcanton et al. (2012), with the exceptions listed in Table 1. We again used the drizzled *HST* WFC3 F814W image from November 2013 as the reference. Although DOLPHOT has a built-in routine for aligning images, it was necessary to calculate initial pixel offsets using the TWEAKREG task in the DRIZZLEPAC package for the images taken on a different epoch (Feb 2014) than the reference. The RMS alignment residuals for the different images ranged from $0''.003$ for the UVIS F555W and F814W images to $0''.03$ for the UV images, and $0''.16$ for the IR images. We also performed aperture photometry with the PHOT task in IRAF. The aperture corrections were calculated using the *HST* PSF models from TINY TIM (Krist 1995; Krist et al. 2011)⁵.

The closest source found by DOLPHOT at I-band is $0''.04$ from the expected position of SN 1997bs with a centroid uncertainty estimated from the reported S/N of the detection of $0''.004$. We also estimate the uncertainty by bootstrap resampling the set of six F814W images that are coadded to form the reference image. The RMS in the location of the closest source to the position of SN 1997bs using these different reference images is $0''.11$. The RMS of the source location found using DOLPHOT with slightly different sets of parameters is $\sim 0''.03$. Taken together, these uncertainties mean that the source position is consistent with the position of SN 1997bs. The photometry for the ACS/WCS images was

² <http://irsa.ipac.caltech.edu/data/SPITZER/docs/dataanalysis/tools/mopex/>

³ IRAF is distributed by the National Optical Astronomy Observatory, which is operated by the Association of Universities for Research in Astronomy (AURA) under cooperative agreement with the National Science Foundation.

⁴ <http://americano.dolphinsim.com/dolphot/>

⁵ <http://tinytim.stsci.edu/cgi-bin/tinytimweb.cgi>

Table 1. DOLPHOT Parameters

Description	Parameter	WFC3/UVIS	WFC3/IR
Photometry aperture radius	RAper	4	3
Inner sky radius	RSky0	15	8
Outer sky radius	RSky1	35	20
χ -statistic aperture size	RChi	2	1.5
Sky Fit	FitSky	1	1
Spacing for sky measurement	SkipSky	2	2

Only parameters differing from those used by Dalcanton et al. (2012) are listed here.

found by again running DOLPHOT with the same reference image. We report the DOLPHOT photometry of the *HST* data in Table 2.

We also looked for an IR source at the position of SN 1997bs. First we registered the *Spitzer* images to the *HST* data using the GEOMAP task in IRAF with coordinates of matched point sources. The point sources were identified by subtracting *Spitzer* images convolved with a larger kernel from those convolved with a smaller kernel. The RMS in the astrometric solution is $\sim 0''.12$. There is no clear point source at the position of SN 1997bs in the *Spitzer* data but we give upper limits based on aperture photometry in Table 2. Unfortunately SN 1997bs is coincident with diffuse IR emission from a spiral arm, making photometric measurements challenging. In order to minimize contamination from diffuse emission and other sources we use a $1''.2$ radius aperture with a $1''.2 - 3''.6$ radius sky annulus together with empirically-determined aperture corrections. While such a small sky annulus includes significant point source flux, the background is non-uniform on larger scales. We also measure the variability of SN 1997bs in the *Spitzer* images taken between 2004 and 2014 using image subtraction. While the $3.6\ \mu\text{m}$ flux stays constant, the $4.5\ \mu\text{m}$ flux declines by $24\ \mu\text{Jy}$.

We use the *LBT* data to place limits on optical variability at the coordinates of SN 1997bs. No source is detected at the position of SN 1997bs and with a dozen epochs spanning 2008-2014 we find slopes consistent with zero in all filters (-110 ± 310 , 60 ± 290 , -370 ± 180 , and $-30 \pm 180\ \text{L}_\odot\text{yr}^{-1}$ and with rms residuals of 1400, 2500, 1500, and $1400\ \text{L}_\odot$ in U, B, V, and R respectively). The new *HST* observations reveal that the F555W luminosity at the position of 97bs decreased $\sim 1.1 \pm 0.3$ mag between 2001 and 2013 and the F814W luminosity decreased $\sim 0.7 \pm 0.2$ mag between 2009 and 2013. In principle the *HST* data can place more stringent limits on variability of the source due to the longer baseline and better resolution, but in practice the *LBT* variability limits may be more reliable and less susceptible to systematic errors by virtue of coming from a single instrument and using image subtraction.

2.3 Confusion

Since we are considering a faint source in a crowded field, we must evaluate the likelihood that our detected *HST* source could be an incidental detection of an unrelated source. We find that the surface density of all DOLPHOT sources within $0''.8$ of the position of SN 1997bs is $31/\text{arc-sec}^2$, which cor-

responds to a 15% chance of an unrelated source being detected within $0''.04$ (the distance of the closest source from the SN location) by chance. For sources as bright (in F814W) as the detection, the surface density is $7/\text{sq-arcsec}$, which reduces the chance of confusion to 4%. However, aperture photometry seems to indicate that confusion is more substantial, with $\sim 30\%$ of apertures laid out over a $0''.8$ grid surrounding the source yielding fluxes as bright as our detection. The large difference between the two methods might be due to DOLPHOT limiting detections to only nearly point-like objects or from source deblending.

Another possibility is that the detection is a surviving companion to the progenitor of SN 1997bs. Massive stars have a large multiplicity fraction ($> 82\%$) (Chini et al. 2012). Kochanek (2009) estimates the magnitude distribution of surviving companions of ccSNe for a set of progenitor masses assuming a uniform distribution of mass ratios. Unfortunately, the mass of the progenitor of SN 1997bs is not well-constrained, but out of the four progenitor models calculated, the progenitor's $m_{F555W} = 22.86$ is most consistent with the $20M_\odot$ model. For this progenitor mass and assuming a binary fraction of 80% there is very roughly a 5-20% chance that there would be a surviving companion to SN 1997bs brighter than our detection. However, as discussed in Kochanek (2009), most secondaries of exploding stars are fainter, blue main sequence stars, but our detection is relatively red ($V - I \sim 1.4$) and would correspond to $T_* \sim 4400\ \text{K}$ if the SED is not strongly influenced by dust. This reduces the likelihood that the detection is a surviving companion.

For the *Spitzer* data the variability in the $4.5\ \mu\text{m}$ flux strongly suggests that the $4.5\ \mu\text{m}$ flux observed in 2004 is associated with SN 1997bs. The IR flux remaining in 2013/14 may be only due to diffuse emission coincident with the original source.

2.4 Basic Scalings for Dust

A common picture of SN impostors is that a surviving star is obscured by a dusty shell ejected at the time of the transient. For such a model, geometry dictates that at late times the evolution of the optical depth of a uniform shell expanding at a constant velocity is $\tau(t) \propto t^{-2}$, where t is the time elapsed since the ejection of the shell. The observed visible light is dominated by scattered photons rather than direct emission, so inhomogeneities in the shells have less effect than naively expected (see Kochanek et al. 2012). Since any inhomogeneities will grow with time, they can only accelerate the optical depth evolution, which would further strengthen

Table 2. Photometry

Filter	Magnitude	Epoch
HST WFC3/UVIS F275W	> 24.7	2014-02-08
HST WFC3/UVIS F336W	26.72 ± 0.69	2014-02-08
HST WFC3/UVIS F438W	27.13 ± 0.35	2014-02-08
HST WFC3/UVIS F555W	26.90 ± 0.15	2013-11-28, 2014-02-08
HST WFC3/UVIS F814W	25.49 ± 0.12	2013-11-28, 2014-02-08
HST WFC3/IR F110W	23.83 ± 0.04	2013-11-28
HST WFC3/IR F160W	22.64 ± 0.04	2013-11-29
SST IRAC 3.6 μm	> 18.2 (< 15 μJy)	July 2013, Feb-Mar-Aug 2014
SST IRAC 4.5 μm	> 18.5 (< 7 μJy)	July 2013, Feb-Mar-Aug 2014
SST IRAC 5.8 μm	> 15.1 (< 109 μJy)	May 2004
SST IRAC 8.0 μm	> 12.5 (< 645 μJy)	May 2004
SST IRAC 3.6 μm	> 18.2 (< 15 μJy)	May 2004
SST IRAC 4.5 μm	> 16.9 (< 31 μJy)	May 2004
HST ACS/WFC F435W	26.78 ± 0.17	2004-12-31
HST ACS/WFC F555W	25.97 ± 0.17	2009-12-14
HST ACS/WFC F814W	24.81 ± 0.10	2009-12-14
HST WFPC2 F555W	25.8 ± 0.3 ^a	2001-03-04
HST WFPC2 F814W	> 25.0 ^a	2001-02-24, 2001-05-28

^aPhotometry taken from Li et al. (2002)

Magnitudes listed with uncertainties are from DOLPHOT PSF photometry.

Magnitudes with only upper limits are from aperture photometry.

our arguments. The evolution of the optical depth in turn must result in a change in the observed luminosity (in a given filter). Consequently, the limits on the observed variability of a source surrounded by an expanding shell can be used to constrain the current effective absorption optical depth, $\tau_{\text{eff}} = [\tau_{\text{abs}}(\tau_{\text{abs}} + \tau_{\text{sca}})]^{1/2}$, where τ_{abs} and τ_{sca} are the absorption and scattering optical depths, by

$$\tau_{V,\text{eff}} < \frac{1}{2} \frac{t}{L_{V,\text{obs}}} \left(\frac{dL_{V,\text{obs}}}{dt} \right), \quad (1)$$

where t is again the elapsed time, $L_{V,\text{obs}}$ is the current observed luminosity, and $dL_{V,\text{obs}}/dt$ is the limit on the rate of change in the observed V-band luminosity. Similarly, variability limits constrain the maximum luminosity, $L_{*,V}$, of a star surviving within an expanding shell to

$$L_{*,V} < \frac{1}{2} \frac{t}{\tau_{V,\text{eff}}} \left(\frac{dL_{V,\text{obs}}}{dt} \right) e^{-\tau_{V,\text{eff}}}. \quad (2)$$

Late-time data, in addition to constraining the optical depth of an expanding shell and the luminosity of a surviving star from the observed variability, can also be used to estimate the mass of the shell. The mass of the shell, M_{ej} , is related to the total optical depth, $\tau_{V,\text{tot}}$, by

$$M_{\text{ej}} = \frac{4\pi v_e^2 t^2 \tau_{V,\text{tot}}(t)}{\kappa_V}, \quad (3)$$

where v_e is the radial velocity of the shell and κ_V is the opacity at V-band. The total and effective optical depths are related by the albedo w with $\tau_{\text{eff}} = (1 - w)^{1/2} \tau_{\text{tot}}$.

Another case to consider is that the progenitor star is obscured by a steady-state dusty wind. We can estimate the mass loss rate needed to obscure the progenitor star with such a wind. If we assume that all of the dust forms at the dust formation radius, R_f , then the rate of mass loss is:

$$\dot{M} = \frac{4\pi v_w R_f \tau_{V,\text{tot}}}{\kappa_V} \quad (4)$$

where $R_f \sim L^{1/2}/T_f^2$ and $T_f \sim 1500$ K is the dust formation temperature. More precisely the dust begins to form at R_f , where the temperature is low enough for grain condensation at a rate proportional to density. As discussed in Kochanek (2011b), R_f has a complex temperature dependence, but would only range from 2.3×10^{14} cm for a $10^{4.7} L_\odot$, 7500 K star to 2.8×10^{15} cm for a $10^{5.4} L_\odot$, 20,000 K star. The dust opacity depends on the distribution of grain sizes and the dust-to-gas ratio, but will generally be within a factor of 2 of 100 cm²/g (of gas) at V-band.

We will utilize these relations in §3.1 and §3.2 to help determine whether a surviving star to SN 1997bs could be obscured by an expanding shell or steady-state wind.

2.5 DUSTY

We model the SED of the source using DUSTY (Ivezic & Elitzur 1997; Ivezic et al. 1999; Elitzur & Ivezić 2001), a code for solving radiative transfer through a spherically symmetric dusty medium. We use stellar atmospheric models from Castelli & Kurucz (2004) for stars of various temperatures and solar composition. We find best-fit models using a Markov Chain Monte Carlo (MCMC) wrapper around DUSTY for both silicate and for graphitic dust from Draine & Lee (1984) using a standard MRN grain size distribution ($dn/da \propto a^{-3.5}$ with $0.005 \mu\text{m} < a < 0.25 \mu\text{m}$; Mathis et al. 1977). In Appendix A we show that our conclusions are not dependent on this choice for the grain size distribution. Since silicate dust is the type expected to form around more massive stars (like the progenitor of SN 1997bs was believed to be) and the conclusions of the paper are robust to the chosen dust type, we will only present the results for silicate dust. For the MRN grain size distribution of silicate dust $w_V \simeq 0.86$, making $\tau_{V,\text{eff}} \simeq 0.37 \tau_{V,\text{tot}}$. The models assume that a shell with a thickness ($R_{\text{out}}/R_{\text{in}}$) of 2.0 expanding with a velocity of $v_e = 765$ km/s (\pm a factor of two; Smith

et al. 2011) was ejected during the 1997 event. We actively expand R_{in} at this rate since the effects of dust are dominated by R_{in} because optical depth drops as R^{-1} . We also produce models for a dusty wind by setting R_{in} equal to the radius corresponding to a typical dust formation temperature of 1500 K (see, e.g., Kochanek 2014c). The χ^2 used in the MCMC is calculated with the logarithmic (linear) differences between modeled and observed fluxes (or limits) in each filter treated as a detection (or limit) and, for the expanding shell models, between modeled and observed v_e (to place the dust at the R_{in} corresponding to the given dust temperature). When considering all photometric constraints as only upper limits we find the luminosity that results in $\Delta\chi^2 = 4$ compared to having no star.

3 A STAR OBSCURED BY DUST?

We consider whether the progenitor of SN 1997bs could have survived obscured by either an expanding dusty shell or by a steady-state wind. Our candidate late-time detection, like those in earlier studies, is marginal and confusion is a non-trivial issue. Therefore, we will consider a range of interpretations for which observations constitute detections and which are only upper limits. We consider the case of F555W and F814W as detections since detections in these filters have been previously reported (Li et al. 2002; Van Dyk & Matheson 2012). We also consider the case of only F814W as a detection, as this is the filter in which a detection is most convincing visually. We consider the case of F814W and $4.5 \mu\text{m}$ as detections because there was a decline in $4.5 \mu\text{m}$ flux between 2004 and 2014 and this represents a scenario in which there is high obscuration. Finally we consider the case where all of the photometry is treated as upper limits, since the candidate detections are marginal and could be due to confusion.

3.1 Obscuration by an Expanding Shell

First we model our photometry as though a surviving star obscured by an expanding shell is recovered with detections in F555W and F814W but only upper limits in the other filters. We present, as an example, the best-fit SED for this case in Fig. 3. This best-fit SED is more than a factor of four fainter than the luminosity of a progenitor with the same T_* and relies on a large amount of obscuration ($\tau_{V,\text{tot}} = 4.8$) to account for the low optical flux currently observed.

The complete results of our MCMC modeling are shown in Fig. 4. When considering only the latest photometric constraints for each filter (the cases displayed on the left side of Fig. 4), it is possible that the star survived with unchanged luminosity but is cloaked beneath a significant amount of extinction. In the cases where either the F555W and F814W photometry or only the F814W photometry is treated as a detection, the star can be cool with relatively low luminosity and low obscuration or hot with higher luminosity and higher obscuration. The F814W-only case allows a more luminous surviving star than the F555W and F814W case because the models no longer have to fit the shallow slope between the F555W and F814W magnitudes, enabling scenarios with higher optical depths to achieve good fits. In

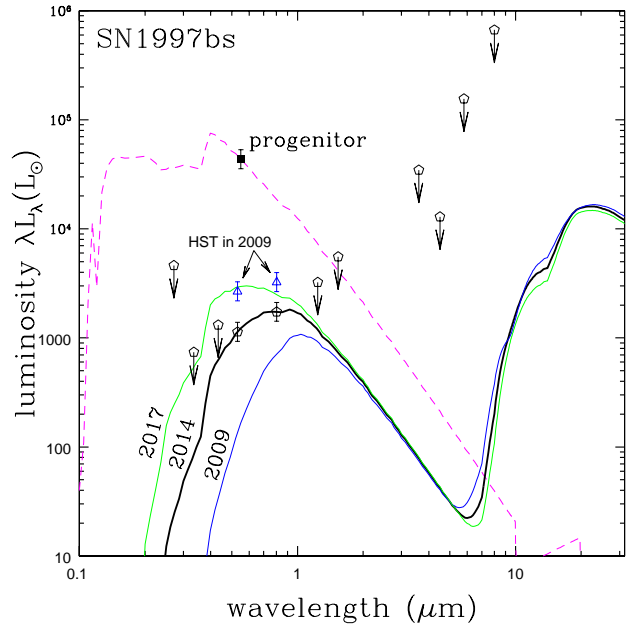


Figure 3. The SED of SN 1997bs with the best-fit model for a silicate shell when treating our F555W and F814W photometry as detections and the other bands as upper limits. The latest *HST* and *SST* detections and limits for a surviving star are shown as the open pentagons with the current best-fit observed model spectrum shown as the thick black line. This best-fit model has $T_* = 11,173$ K, $\tau_{V,\text{tot}} = 4.79$, and $L_* = 10^{4.27} L_\odot$. We also show this best-fit model evolved forwards in time to 2017 in green and backwards in time to 2009 in blue with $\tau \propto t^{-2}$ but with the same T_* and L_* . The tension between the 2009 *HST* photometry, shown as the open blue triangles, with the best-fit shell model evolved back to 2009 illustrates how models in which SN 1997bs is obscured by an expanding dusty shell cannot be reconciled with the late-time optical evolution. For comparison, we show the *HST* progenitor detection as the solid black square and an unobscured model spectrum with $T_* = 11,173$ K as the dashed magenta line.

the F814W and $4.5 \mu\text{m}$ case, a cooler star with lower luminosity and lower obscuration is not allowed by the mid-IR detection, which requires a significant luminosity to be reprocessed by dust. If all of the photometry is taken as only upper limits, the MCMC modeling would be poorly constrained, so we instead show the maximum allowed luminosity of a surviving star for optical depths of $\tau_{V,\text{tot}} = 0, 1, 3$, and 10. The limits-only case echoes the results of the other cases – the latest photometric constraints, taken alone, allow for a luminous, but heavily-obscured, surviving star.

These limits are relatively robust to variations in the velocity of the expanding shell. Doubling the assumed velocity of the expanding shell only significantly increases the maximum luminosity of a surviving star with $T_* \gtrsim 25,000$ K and $\tau_{V,\text{tot}} = 10$ and then only by ~ 0.3 dex. Conversely, halving the expansion velocity decreases the maximum luminosity in the same parameter range by a similar amount.

That solutions consistent with the photometric data exist does not mean they are physical because they may imply unphysical ejecta masses or unobserved variability.

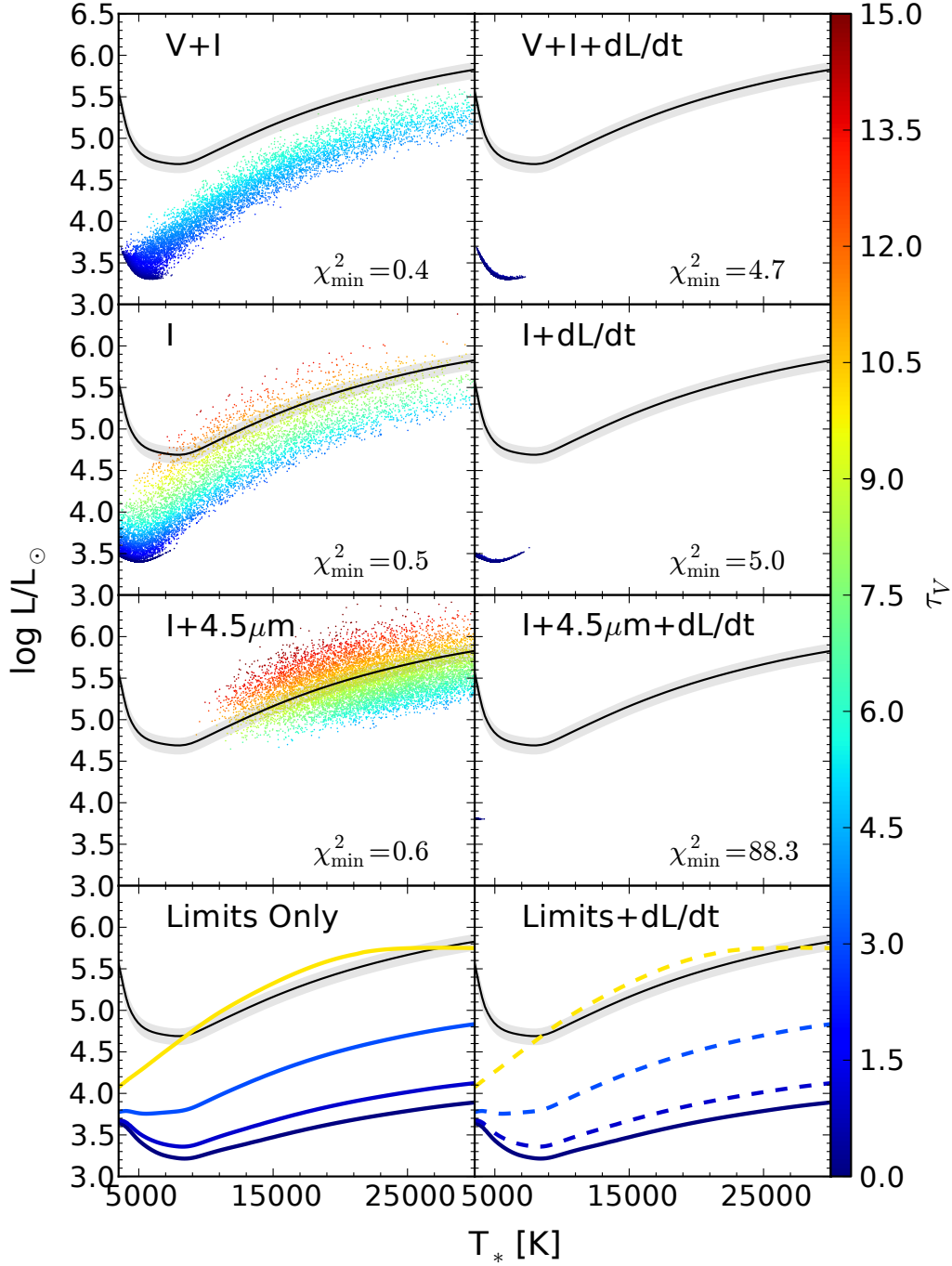


Figure 4. MCMC results for the luminosity and temperature of a surviving star obscured by an expanding shell ejected at the time of the SN 1997bs transient when imposing different possible photometric constraints: treating the *HST* WFC3/UVIS F555W and F814W photometry as detections and the other filters as only upper limits (top row), treating the *HST* WFC3/UVIS F814W photometry as a detection and the other filters as upper limits (2nd row from the top), treating the *HST* WFC3/UVIS F814W and *SST* 4.5 μm photometry as detections and the other filters as upper limits (2nd row from the bottom), and treating all photometry as upper limits (bottom row). The panels on the right also fold in the constraint from the limit on variability in the *LBT* data (Eqn. 9). The panels on the bottom row show the maximum luminosity possible for a surviving star with an obscuration of $\tau_{V,\text{tot}} = 0, 1, 3$ and 10. The dotted lines indicate luminosities for a given optical depth that are disallowed by the limits on $d\tau/dt$ from the *LBT* observations (Eqn. 9). For comparison, the solid black line and gray band indicates the progenitor luminosity as constrained by the pre-explosion measurement of $m_{F606} = 22.86$ and its $1\text{-}\sigma$ uncertainty (0.16 mag). The lowest χ^2 value for the 10,000 MCMC steps accepted is given for each panel. The panels on the left show that the latest photometric constraints, taken alone, do not rule out the star surviving with its pre-eruption luminosity if obscured by a shell with $\tau_{V,\text{tot}} \gtrsim 5$. However, the panels on the right show that the dL/dt limits rule out an expanding shell of any significant optical depth and only allow a surviving star with a greatly diminished luminosity. The results in the I+4.5 μm + dL/dt panel are difficult to see because they are clustered around 3500 K at $10^{3.8} L_{\odot}$. The *HST* variability limits are even more constraining.

First we consider the ejecta mass needed to obscure a surviving star with an unchanged intrinsic luminosity. Fig. 4 shows that this would require the current optical depth to be $\tau_{V,\text{tot}} \sim 10$. Using Eqn. 3, we find

$$M_{\text{ej}} = 1.0 \left(\frac{v_e}{765 \text{ km/s}} \right)^2 \left(\frac{t}{16.5 \text{ yr}} \right)^2 \times \left(\frac{\tau_{V,\text{tot}}}{10} \right) \left(\frac{100 \text{ cm}^2/\text{g}}{\kappa_V} \right) M_{\odot}. \quad (5)$$

Such an ejected mass is feasible, but, as we shall see, this scenario is inconsistent with the variability constraints dictated by geometric expansion. The kinetic energy of the ejecta, $E_{\text{kin}} = \frac{1}{2} M_{\text{ej}} v_e^2$, in this scenario would be

$$E_{\text{kin}} = 6 \times 10^{48} \left(\frac{v_e}{765 \text{ km/s}} \right)^4 \left(\frac{t}{16.5 \text{ yr}} \right)^2 \times \left(\frac{\tau_{V,\text{tot}}}{10} \right) \left(\frac{100 \text{ cm}^2/\text{g}}{\kappa_V} \right) \text{ erg}. \quad (6)$$

We compare this to the radiated energy, $E_{\text{rad}} = t_{1.5} \zeta L_{\text{peak}}$, of the transient estimated by Smith et al. (2011) of

$$E_{\text{rad}} = 7 \times 10^{49} \left(\frac{t_{1.5}}{45 \text{ days}} \right) \left(\frac{L_{\text{peak}}}{1.2 \times 10^7 L_{\odot}} \right) \zeta \text{ erg}. \quad (7)$$

where L_{peak} is the peak luminosity of the outburst, $t_{1.5}$ is the time for the transient to fade by 1.5 mag from its peak, and $\zeta \sim 1$ is a dimensionless factor that depends on the shape of the light curve. The high ratio of radiated to kinetic energy in this scenario would likely require a radiative, rather than explosive, mechanism.

Fig. 3 also illustrates how the expanding shell model that best fits the latest data would necessarily have been much fainter in the optical in 2009, in gross disagreement with the *HST* photometry from 2009. A model in which $\tau_{V,\text{tot}} = 10$ would be in even more severe conflict with the photometric evolution. More quantitatively, using Eqn. 1 with the 3σ upper limit on the variability from the *LBT* data constrains the current maximum optical depth of an expanding shell to be

$$\tau_{V,\text{eff}} < 1.2 \left(\frac{t}{16.5 \text{ yr}} \right) \left(\frac{1135 L_{\odot}}{L_{V,\text{obs}}} \right) \left(\frac{dL_{V,\text{obs}}/dt}{170 L_{\odot}/\text{yr}} \right). \quad (8)$$

Similarly, we can use the variability limits from *LBT* and Eqn. 2 to constrain the maximum luminosity of a star surviving within an expanding shell as

$$L_{*,V} < 520 \left(\frac{t}{16.5 \text{ yr}} \right) \left(\frac{dL_{V,\text{obs}}/dt}{170 L_{\odot}/\text{yr}} \right) \frac{e^{1-\tau_{V,\text{eff}}}}{\tau_{V,\text{eff}}} L_{\odot}. \quad (9)$$

The effects of these constraints on estimates of the stellar properties are shown in Fig. 4 by the panels on the right. Using the limit on dL/dt from *LBT* together with the *HST* photometry restricts solutions to have low optical depths ($\tau_{V,\text{tot}} \lesssim 1$) and makes it impossible for any shell model to achieve a low χ^2 . Moreover, the putative *HST* source at the coordinates of 97bs seems to have faded between 1998 and 2013, which further rules out an expanding shell of any optical depth.

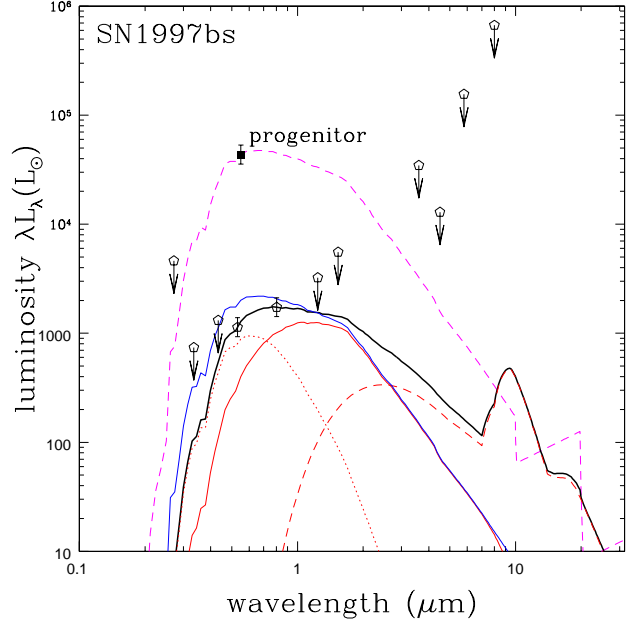


Figure 5. The SED of SN 1997bs with the best-fit model for a silicate wind with an inner edge temperature of $T_f = 1500$ K when treating our F555W and F814W photometry as detections and the other bands as upper limits. The *HST* and *SST* detections and limits for a surviving star are shown as the black open pentagons with the best-fit observed model spectrum shown as the thick black line, the intrinsic input SED is the thin blue line, and the contributions of the attenuated input radiation, scattered radiation, and dust emission are shown as thin red solid, dotted, and dashed lines respectively. This particular model has $T_* = 5093$ K, $\tau_{V,\text{tot}} = 1.61$, and $L_* = 3014 L_{\odot}$. For comparison, we show the *HST* progenitor detection as the solid black square and a model spectrum also with $T_* = 5093$ K as the dashed magenta line.

3.2 Obscuration by a Wind

Rather than being obscured by a dusty shell ejected during the outburst in 1997, the surviving star could be obscured by a steady-state dusty wind that began following the transient. For our standard models we adopt an inner (dust formation) temperature of $T_f = 1500$ K. We present, as an example, the best-fit SED for a wind when treating our F555W and F814W photometry as detections and the other bands as upper limits in Fig. 5. The striking fact is that the luminosity of the best-fitting SED for our candidate detection is fainter than the progenitor by more than a factor of 20 when modeled as being obscured by a dusty wind.

The complete MCMC results are shown in Fig. 6. The *HST* F110W and F160W photometric limits strongly constrain the amount of hot dust around the source. As a result, at least for the cases where only optical filters are treated as detections, a surviving star is constrained to be cool with low to moderate obscuration ($\tau_{V,\text{tot}} \lesssim 6$) and a significantly lower luminosity than the progenitor. While the case where the F814W and $4.5 \mu\text{m}$ photometry are treated as detections appears to favor a heavily obscured source with only slightly lower luminosity than the progenitor, all of the models in this case have high χ^2 values because of the great difficulty in accounting for the $4.5 \mu\text{m}$ flux with $T_f = 1500$ K without

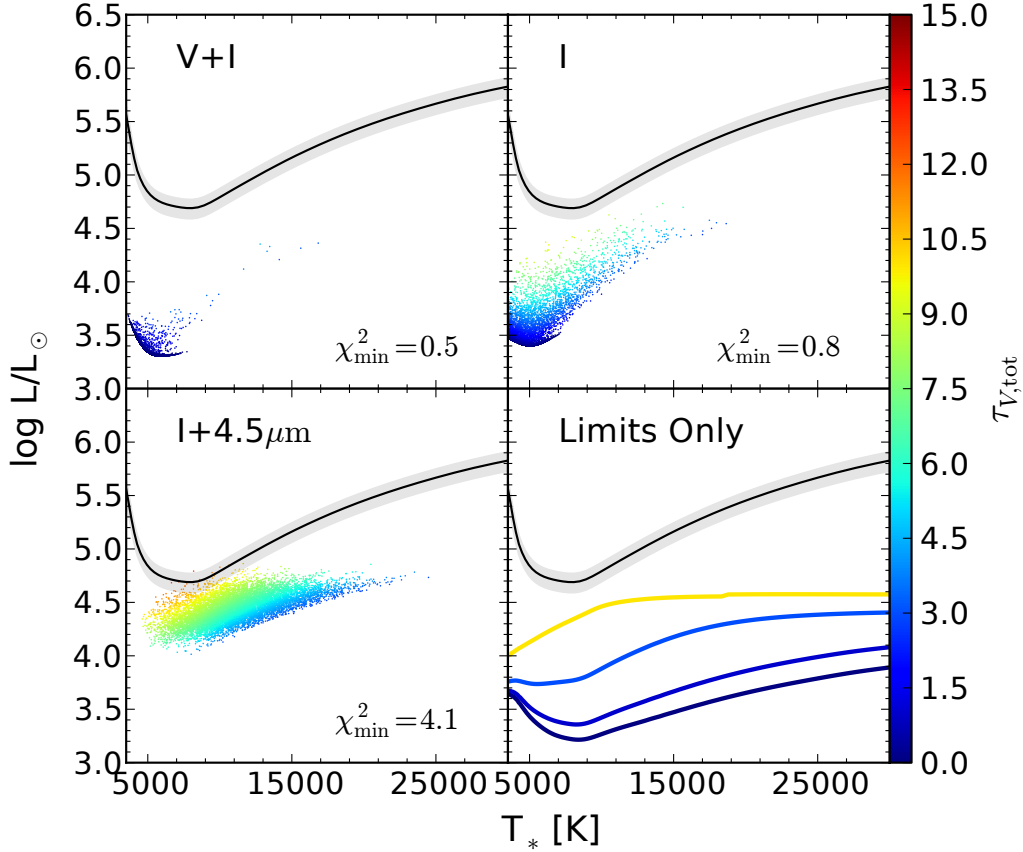


Figure 6. MCMC results for the luminosity and temperature of a surviving star obscured by a steady-state wind when imposing different possible photometric constraints: treating the *HST* WFC3/UVIS F555W and F814W photometry as detections and the other filters as only upper limits (top left), treating the *HST* WFC3/UVIS F814W photometry as a detection and the other filters as upper limits (top right), treating the *HST* WFC3/UVIS F814W and *SST* 4.5 μm photometry as detections and the other filters as upper limits (bottom left), and treating all photometry as upper limits (bottom right). The lines in the “limits only” panel show the maximum luminosity possible for a surviving star with an obscuration of $\tau_{V,\text{tot}} = 0, 1, 3$, and 10. For comparison, the solid black line and gray band indicates the progenitor luminosity as constrained by the pre-explosion measurement of $m_{F606} = 22.86$ and its $1\text{-}\sigma$ uncertainty (0.16 mag). The lowest χ^2 value for the 10,000 MCMC steps accepted is given for each panel. Well-fit wind models are possible when treating the F555W and F814W photometry as detections, but these models require a surviving star to be much fainter than the progenitor. Though the panel where both the F814W and the 4.5 μm photometry are treated as detections appears to allow a luminous survivor, these models have a high χ^2 because of the great difficulty in accounting for the 4.5 μm flux with $T_f = 1500$ K dust without violating the *HST* near-IR limits. It is very unlikely that a surviving star is obscured by a steady-state wind unless the star is significantly fainter than the progenitor.

violating the *HST* near-IR limits. When we model all of the photometry as upper limits (see the lower-left panel in Fig. 6) we see that $\tau_{V,\text{tot}} > 10$ is needed to allow the star to survive with an undiminished luminosity behind a dusty wind. As illustrated by the high χ^2 values of the case where the F814W and 4.5 μm photometry are treated as detections, such a high optical depth is only possible if all the optical constraints are only upper limits.

These limits are relatively robust to variations in the assumed dust condensation temperature in the wind. Models of a steady-state wind with cooler dust condensation temperatures result in slightly weaker luminosity limits for a hot, heavily-obscured surviving star. Even if we drop the condensation temperature to $T_f = 1000$ K (750 K) the luminosity limit for a $T_* > 7500$ K surviving star with $\tau_{V,\text{tot}} = 10$ only increases by ~ 0.3 dex (~ 0.5 dex). We note, however, that setting $T_f = 1000$ K significantly improves the fit of the

model ($\chi_{\text{min}} = 0.9$) in the case where F814W and 4.5 μm are treated as detections by easing the tension with the near-IR flux limits.

We can use Eqn. 4 to estimate the mass loss rate required to achieve $\tau_{V,\text{tot}} \sim 10$. Using the observed ejecta velocity of SN 1997bs as v_w , the mass loss rate would correspond to $3 \times 10^{-4} M_\odot \text{ yr}^{-1}$ ($4 \times 10^{-3} M_\odot \text{ yr}^{-1}$) for a $10^{4.7} L_\odot$ ($10^{5.4} L_\odot$), 7500 K (20,000 K) star. Such high mass loss rates are typical of active LBVs (Puls et al. 2008), although a still higher mass loss rate of $\gtrsim 10^{-2.5} M_\odot \text{ yr}^{-1}$ is needed in order for dust formation to occur around hot ($T \gtrsim 10,000$ K) stars (Kochanek 2011b, 2014c). Additionally, at their these high mass loss rates, the wind itself becomes optically thick independent of any dust leading to a pseudophotosphere with an apparent temperature of $T \sim 7000$ K (Davidson 1987).

A mass loss rate of $\dot{M} > 10^{-2.5} M_\odot / \text{yr}$ would cor-

respond to $\tau_{V,\text{tot}} > 140$ (12) for $T_* = 7500$ K (20,000 K). Essentially this means that for a hot surviving star there must be either no dust in the wind or a very thick dusty wind ($\tau_{V,\text{tot}} > 12$). Even allowing optical depths as high as $\tau_{V,\text{tot}} = 1000$ while treating all of our photometry as upper limits only allows a surviving star with $L_* < 10^{4.6} L_\odot$, which is still slightly less than the minimum luminosity of the progenitor. Moreover, $\tau_{V,\text{tot}} \gg 10$ is inconsistent with any optical detection of a source. An extremely high optical depth would require the candidate F555W and F814W detections reported here, by Li et al. (2002), and by Van Dyk & Matheson (2012) to be the result of confusion, even though the source appears to be fading.

4 DISCUSSION

The new *HST* images we present clearly lack a source with optical flux comparable to the progenitor of SN 1997bs. If SN 1997bs was a non-terminal event the diminished optical flux could be due to increased obscuration of the star, an increase in the star’s temperature, or an intrinsic decline in the luminosity. The alternative is that SN 1997bs was a genuine SN. We evaluate these different scenarios and the limits placed on them by the data.

4.1 Obscuration

The late-time photometric evolution of SN 1997bs is grossly inconsistent with the prevailing notion of it being a supernova impostor in which a non-terminal eruption ejected a significant amount of mass that then obscured the surviving star. The observed limits on the variability at the position of SN 1997bs from *HST* and *LBT* rule out any expanding dusty shell scenario (see the right-side panels of Fig. 4).

The new data also rule out the alternative, a steady dusty wind, which Kochanek et al. (2012) found was consistent with earlier archival data (see Fig. 6). The high mass loss rate needed for self-shielding so that dust can form in the wind of a hot ($T_* \gtrsim 10,000$ K) star would result in a large $\tau_{V,\text{tot}}$ that would not allow the candidate optical detections reported here and by Li et al. (2002) and Van Dyk & Matheson (2012).

4.2 Bolometric Correction

If we assume there is no dust obscuration, the maximum luminosity of the surviving star is $\sim 10^{4.1} L_\odot$ (see the $\tau_{V,\text{tot}} = 0$ line in the “Limits Only” panel of Fig. 4 or 6), which is significantly fainter than the traditional range of luminosities for LBVs. It is unlikely that the low luminosity could solely be the result of a large bolometric correction. Allowing a surviving star to have an effective temperature of up to 40,000 K, the maximum luminosity of a surviving star is still at least a factor of four fainter than the minimum luminosity of the progenitor. For temperatures higher than 40,000 K, the maximum luminosity of the star can be constrained by the maximum possible H β flux allowed by our F555W photometry, since a very luminous hot star would produce a significant flux of ionizing photons and the ejecta would provide an absorbing medium. If we assume the star emits a blackbody spectrum and is surrounded by enough

gas to absorb the photons with 11% of recombinations going through the H β branch (based on Case B recombination coefficients for $T_* = 20,000$ K from Draine (2011)) and set the H β flux equal to our flux limit for F555W (we do not use H α because its wavelength places it in the tail of the F814W filter response curve), we find the maximum luminosity of a $T_* = 40,000$ K star is $\sim 10^{5.0} L_\odot$, with lower maximum luminosities for increasing T_* . Accordingly, we cannot completely rule out the possibility that a progenitor initially with $4400 \lesssim T_* \lesssim 13,000$ K survived the episode as a $T_* > 40,000$ K Wolf-Rayet star. However, it seems unlikely that a single short duration event could affect such a dramatic change.

4.3 A Tuckered-Out Star

The only remaining possibility that would allow SN 1997bs to be a non-terminal event is that the progenitor survived the event with a diminished luminosity – the “tuckered-out” star hypothesis (Smith et al. 2011). If a surviving star is unobscured and its temperature is unchanged from pre-eruption, it must be at least a factor of ~ 30 fainter than the progenitor. No known mechanism could so drastically diminish the intrinsic luminosity of the star. As mentioned in the previous section, even if we allow for a significant increase in the temperature of the star, a factor of four decrease in the luminosity is required by the latest observations. A conspiracy of factors could explain the dramatic drop in apparent luminosity. Though an expanding dusty shell is ruled out by limits on the observed variability, a combination of a steady-state dusty wind and a significant increase in T_* could allow for a surviving star with a luminosity that has declined by as little as $\sim 25\%$. However, this collusion is disfavored by the candidate late-time detections of an optical source.

The ‘buildup’ or ‘recovery’ time-scale for the radiated energy budget given by Smith et al. (2011) is $t_{\text{rad}} = E_{\text{rad}}/L_* = t_{1.5}\zeta L_{\text{peak}}/L_*$, where E_{rad} is the energy radiated during the outburst, L_{peak} is the peak luminosity of the outburst, L_* is the quiescent pre-outburst luminosity of the progenitor, and ζ is a dimensionless factor. For SN 1997bs this is

$$t_{\text{rad}} \sim 27 \left(\frac{t_{1.5}}{45 \text{ days}} \right) \left(\frac{L_{\text{peak}}/L_*}{220} \right) \zeta \text{ yr}, \quad (10)$$

which means that a large fraction of this recovery time-scale has already elapsed with no re-brightening of a surviving star.

This time-scale may not be the most relevant time-scale for the stellar luminosity, since the envelope would likely return to thermal equilibrium primarily through Kelvin-Helmholtz contraction rather than by energy radiated from the core. In order to decrease the bolometric luminosity for such an extended period of time either some of the nuclear energy generated must be diverted into gravitational potential energy by inflating the stellar envelope or the nuclear luminosity must have decreased.

If the missing luminosity is being used to alter the structure of the outer layers of the star, the time-scale for it to lift mass ΔM against the gravitational potential of the star

is

$$t_{\text{infl}} \sim 120 \left(\frac{\Delta M}{M_{\odot}} \right) \left(\frac{M_{*}}{20 M_{\odot}} \right) \left(\frac{T_{*}}{10,000 \text{ K}} \right)^2 \times \left(\frac{L_{*}}{10^5 L_{\odot}} \right)^{-3/2} \left(\frac{0.5}{f} \right) \text{ yr}, \quad (11)$$

where M_{*} , T_{*} , and L_{*} are the mass, temperature, and luminosity of the progenitor, and f , is the fraction by which the radiated luminosity has decreased. This could account for the missing energy, but it is unclear if there is a theoretical mechanism that could drive this. Moreover, t_{infl} is not so long that we would expect no external changes on time-scales of a decade. Another problem is that the most natural post-eruption state would be a star with an over-expanded envelope rather than the reverse. The envelope would then shrink on a thermal time-scale, rapidly at first but then slowing, making the star overluminous, not subluminal. The over-expansion is a natural consequence if any transient mechanism which has no “knowledge” of the escape speed and has mainly been discussed in the context of shock-heating non-degenerate companions of Type Ia SNe (Shappee et al. 2013; Pan et al. 2013).

The final alternative is for the nuclear luminosity to have decreased. The core luminosity should be unaltered as it can only change over a (core) thermal time-scale, but it might be possible for the luminosity from shell-burning to decrease suddenly in certain (fine-tuned) situations. Perhaps the progenitor had previously experienced enough mass loss for its hydrogen-burning shell to be close to its surface and the star experienced a final shell flash, analogous to the final shell flash of an AGB star. If the progenitor was very massive star ($M_i \gtrsim 80 M_{\odot}$), a thermonuclear outburst from pulsational pair instability might be another possibility (Woosley & Heger 2015).

4.4 SN and Confusion

Alternatively, SN 1997bs could have been a terminal event. If the star went supernova, our detection of a $F814W = 25.49 \pm 0.12$ source $0^{\circ}016$ from the position of SN 1997bs must be due to confusion, a surviving companion, or the supernova ejecta. As we describe in §2.3, the likelihood of our detection being due to confusion is between 4% and 30%. The likelihood of the source being a surviving binary companion is comparable, at 5-20%, although we would expect a surviving companion to be bluer. The slight decrease in luminosity between the 2001 *HST*/*WFPC2*, 2009 *HST*/*ACS*, and 2013 *HST*/*WFC3* F555W and F814W images reduce the likelihood that the detection is due to confusion, although there could be systematic issues in comparing the crowded field photometry based on the three different instruments.

The $4.5 \mu\text{m}$ flux measured at the location of SN 1997bs dropped from a significant $31 \pm 4 \mu\text{Jy}$ in 2004 to $7 \pm 3 \mu\text{Jy}$ in 2014. This variability indicates that the $4.5 \mu\text{m}$ flux observed in 2004 originated from SN 1997bs and is not confusion. The decrease in the $4.5 \mu\text{m}$ flux while the $3.6 \mu\text{m}$ flux stayed constant is difficult to explain if the $3.6 \mu\text{m}$ flux is from SN 1997bs. More likely, the $3.6 \mu\text{m}$ flux is unrelated to SN 1997bs (SN 1997bs is close to a spiral arm) and the

decreasing $4.5 \mu\text{m}$ emission was from warm ($\sim 1000 \text{ K}$) dust that has since cooled.

It is possible that we are detecting residual flux from the shock interaction of SN 1997bs with its circumstellar medium. If we parameterize the fraction of the maximum possible shock luminosity radiated in our observed filters as f , then the observed shock luminosity is given by

$$L_{s,\text{obs}} \simeq 2.3 \times 10^3 \left(\frac{\dot{M}}{10^{-4} M_{\odot}} \right) \left(\frac{v_e}{765 \text{ km/s}} \right)^3 \times \left(\frac{v_w}{100 \text{ km/s}} \right)^{-1} \left(\frac{f}{0.1} \right) L_{\odot} \quad (12)$$

where \dot{M} is the pre-eruption mass loss rate, v_e is the velocity of the SN ejecta, and v_w is the pre-eruption wind velocity. Although we do not have constraints on \dot{M} or v_w since little is known about the progenitor, reasonable values of v_w and f , together with a relatively (but not outrageously) high \dot{M} during the decades preceding the transient, are sufficient to possibly account for our detection ($\sim 1700 L_{\odot}$ in F814W).

It is worth reconsidering why SN 1997bs was originally designated as a likely SN impostor: a low peak luminosity and a possible flattening of the late-time ($\gtrsim 250$ days post-explosion) light curve at ~ 0.5 mag fainter than the progenitor (see Van Dyk et al. 1999). However, the source at the coordinates of SN 1997bs, rather than re-brightening as required if obscured by an expanding dusty shell, has only continued to fade and is now ~ 4 mag fainter than the progenitor. For the most likely physical conditions, the near-IR limits rule out the star surviving in a dusty wind. Thus, it is very difficult to reconcile late-time observations of 97bs with the prevailing notion that it was a non-terminal eruption.

SN 1997bs can be explained as a low energy supernova. Over the last two decades, a class of faint Type IIP SNe has emerged with peak magnitudes as faint as $M_V = -13.76$ (SN 1999br; Pastorello et al. 2004), less than a magnitude brighter than 97bs ($M_V \sim -12.9$). These faint SNe have low ejected ^{56}Ni masses ($\sim 10^{-3} M_{\odot}$) and require low explosion energies ($L < 10^{51}$ ergs). The low ^{56}Ni mass is likely due to fall-back of material onto the collapsed remnant (see e.g., Woosley & Weaver 1995). Although the late-time light curve of SN 1997bs might have significant contributions from a CSM-SN shock interaction, we can estimate the maximum ^{56}Ni mass ejected by scaling the V-band luminosity to that of the well-studied faint IIP SN 1997D at the same epoch (270 days post-explosion). Nominally this would suggest that the maximum ^{56}Ni mass for 97bs is 20 times smaller than the $0.002 M_{\odot}$ estimated for SN 1997D by Turatto et al. (1998). However, 97bs was much redder than 97D by this point ($V - I \sim 4.5$ vs ~ 1.2 mag) and was likely significantly obscured. If we posit that extinction is needed to match the colors, then 97bs had $E(B - V) \sim 2.3$ mag at this point, which would increase the maximum ^{56}Ni mass by nearly a factor of 1000. Even if the shock luminosity contributed a large fraction of the luminosity, 97bs could still potentially have more ejected ^{56}Ni than a significant fraction of faint IIP's.

Thus, SN 1997bs could be a IIn analog of a faint IIP. Progenitor detections and hydrodynamical modeling of light curves point to faint IIP SNe progenitor masses of $10\text{--}15 M_{\odot}$ (Spiri et al. 2014). Meanwhile, recent work in SN theory by Ugliano et al. (2012) and Pejcha & Thompson (2014)

suggests that stars with masses between 14-16 M_{\odot} , some between 17-22 M_{\odot} , and stars between 23-26 M_{\odot} are the most difficult to explode. Faint IIP SNe might arise from the lower mass (14-16 M_{\odot}) stars that have density structures resulting in low energy explosions while 97bs and similar “impostors” could arise from the higher mass (23-26 M_{\odot}) stars. These higher mass stars have the potential to have the pre-explosion mass loss required for a transient to have the narrow hydrogen emission lines that are characteristic of SN IIn (and SN impostor) spectra.

The event could even be a collapse-induced thermonuclear supernova (Kushnir & Katz 2014), which would dump enough energy in the stellar envelope quickly enough to drive a shock in a manner similar to the piston simulations of Dessart et al. (2010). This would be a weak, terminal event of a star in one of the harder-to-explode mass ranges.

All of these low energy explosions are also much more favorable for dust formation because condensation will occur at much higher densities (see, e.g., Kochanek 2014b). This would provide a natural explanation of the increasingly red colors observed by Van Dyk et al. (2000), since dust formation fairly naturally correlates with dropping luminosity. The lack of a surviving star then avoids the problems with dusty models of a surviving star.

4.5 Summary

Our late-time observations of SN 1997bs seem most easily understood if SN 1997bs was, in fact, the first SN found by LOSS. It is somewhere between difficult and impossible to explain the data as dust obscuration by either an expanding shell or a wind for a star with the luminosity of the progenitor at any temperature. Similarly, invoking bolometric corrections or simply making the star less luminous seems difficult to support. Occam’s razor, if nothing else, argues for simply making it an SN rather invoking a more baroque model.

Nature does not, of course, have to respect Occam’s razor. Further observations are necessary to confirm the fate of SN 1997bs. Unfortunately it is impossible to resolve any IR emission from SN 1997bs with the diffuse emission from the nearby spiral arm with *Spitzer*. The improved resolution and sensitivity of the *James Webb Space Telescope* is needed to reduce the mid-IR limits enough to completely rule out a cool star behind a thick, dusty wind.

As argued by Kochanek et al. (2012), the current class of SN impostors is likely comprised of multiple phenomena. We find that SN 1997bs, an archetypal SN impostor, was likely a genuine SN, but there are also several SN impostors that have clearly undergone multiple non-terminal outbursts (e.g., SN 2000ch, 2002kg, 2009ip). Moreover, in newly obtained *HST* images, we confirm a surviving star to the SN impostor 1954J, as proposed by Smith et al. (2001) and Van Dyk et al. (2005) (Adams & Kochanek 2015 in prep.). At least a significant fraction of SN impostor progenitors are relatively low ($15 M_{\odot} < M < 25 M_{\odot}$) stars (Smith et al. 2011; Kochanek et al. 2012). These masses are lower than the mass range of “classical” LBVs and should not be close to their Eddington limits and any of the radiative instabilities of classical LBVs. Recurrent impostors have the highest progenitor masses (see Table A1). Perhaps some of the lower mass impostors are faint IIn SNe and only the impostors

Table A1. SN Impostor Masses

Object	$M_i[M_{\odot}]$
Single Episode	
SN 2008S	$\sim 10^a$
2008-OT	12 – 15 ^a
SN 1997bs	12 – 24 ^a , > 20 ^b
SN 2003hm	14 – 17 ^a , > 20 ^b
SN 1954J	14 – 21 ^a , > 20 ^b
2009-OT	$\sim 25^b$
HD 5980	58 – 79 ^{c*}
SN 1961V	> 80 ^d
Reccurent	
P Cygni	20 – 40 ^{e*}
SN 2002kg	> 15 ^a , > 40 ^b
SN 2000ch	20 – 80 ^a , > 40 ^f
SN 2009ip	50 – 80 ^b
η Car	$\sim 160^g$

*Current mass

^aKochanek et al. (2012)

^bVan Dyk & Matheson (2012)

^cFoellmi et al. (2008)

^dKochanek et al. (2011)

^eLamers et al. (1983)

^fWagner et al. (2004)

^gDavidson & Humphreys (1997)

arising from more massive stars are non-terminal eruptions of LBVs.

ACKNOWLEDGEMENTS

We thank Jill Gerke for providing the LBT variability limits, Andrew Dolphin for assistance with DOLPHOT, and Rubab Khan, Marc Pinsonneault, José Prieto, Kris Stanek, and Todd Thompson for discussions and comments. This work is based in part on observations made with the Spitzer Space Telescope, which is operated by the Jet Propulsion Laboratory, California Institute of Technology under a contract with NASA, and in part on observations made with the NASA/ESA *Hubble Space Telescope* obtained at the Space Telescope Institute, which is operated by the Association of Universities for Research in Astronomy, Inc., under NASA contract NAS 5-26555. These observations are associated with program GO-13477. This work is also based in part on observations made with the Large Binocular Telescope. The LBT is an international collaboration among institutions in the United States, Italy, and Germany. The LBT Corporation partners are: the University of Arizona on behalf of the Arizona university system; the Istituto Nazionale di Astrofisica, Italy; the LBT Beteiligungsgesellschaft, Germany, representing the Max Planck Society, the Astrophysical Institute Potsdam, and Heidelberg University; the Ohio State University; and the Research Corporation, on behalf of the University of Notre Dame, the University of Minnesota, and the University of Virginia.

APPENDIX A: DUST SIZE DISTRIBUTION

Although the MRN dust size distribution we assumed for the analysis presented in this paper is a reasonably accurate

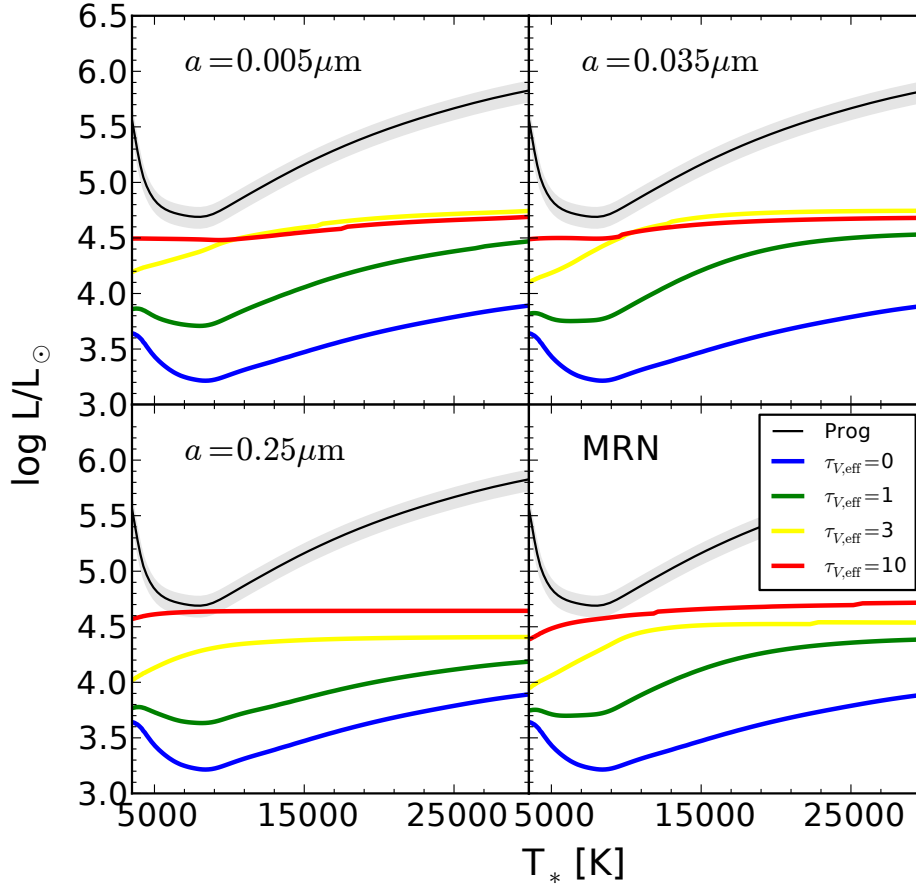


Figure A1. Results for the maximum luminosity possible for a surviving star obscured by a steady-state silicate wind with $\tau_{V,\text{eff}} = 0, 1, 3$, and 10 for different dust grain sizes, a , as compared to the results for an MRN dust size distribution (bottom right panel) when treating all photometry as upper limits. The solid black line and gray band indicates the progenitor luminosity as constrained by the pre-explosion measurement of $m_{\text{F606}} = 22.86$ and its 1- σ uncertainty (0.16 mag).

prescription for the size distribution of interstellar dust, dust formed around a particular star will grow to a particular size that is dependent on the density and radiation field of the circumstellar environment (see, e.g., Kochanek 2014c, for a discussion). Unfortunately, we are unable to determine a most likely dust size, since the size, an input to our models, is dependent on the output (i.e., τ , T_* , and L_*) from the models.

Instead, we evaluated our models for a number of dust sizes ranging from $0.005 \mu\text{m}$ to $0.25 \mu\text{m}$ and verified that our conclusions are robust to the chosen dust size. For an example, in Fig. A1 we present the results of the silicate wind model for a range of dust sizes and effective optical depths. For silicate dust grain sizes, a , of $0.005 \mu\text{m}$, $0.035 \mu\text{m}$, $0.25 \mu\text{m}$, and an MRN size distribution the albedo is $w_V \simeq 0, 0.10, 0.43$, and 0.39 , corresponding to $\tau_{V,\text{eff}} \simeq 1.00, 0.82, 0.32$, and 0.37 respectively. For a given effective optical depth the luminosity limits on a surviving star are largely unchanged. The most significant difference is that the χ^2 of the best fitting model for a silicate wind with our F814 and $4.5 \mu\text{m}$ photometry treated as detections for a dust size of $0.035 \mu\text{m}$ is only 1.3 (compared to 4.1 for an MRN distribution of dust), slightly reducing the confidence with

which we can rule out a luminous star surviving behind a dusty wind.

The impacts of the dust size on the results of the shell model are even more limited. For a given effective optical depth the only significant change for different dust sizes is that the luminosity limit for a cool star with heavy obscuration is increased. The key point, however, is that the dL/dt limits continue to rule out an expanding shell with an optical depth high enough to hid a luminous star for all reasonable dust sizes.

REFERENCES

- Alard C., 2000, A&AS, 144, 363
- Alard C., Lupton R. H., 1998, ApJ, 503, 325
- Bertin E., 2006, in Astronomical Society of the Pacific Conference Series, Vol. 351, Astronomical Data Analysis Software and Systems XV, Gabriel C., Arviset C., Ponz D., Enrique S., eds., p. 112
- Bertin E., Arnouts S., 1996, A&AS, 117, 393
- Bertin E., Mellier Y., Radovich M., Missonnier G., Didelon P., Morin B., 2002, in Astronomical Society of the Pacific Conference Series, Vol. 281, Astronomical Data Analysis

- Software and Systems XI, Bohlender D. A., Durand D., Handley T. H., eds., p. 228
- Botticella M. T., Smartt S. J., Kennicutt R. C., Cappellaro E., Sereno M., Lee J. C., 2012, *A&A*, 537, A132
- Castelli F., Kurucz R. L., 2004, *astro-ph/0405087*
- Chini R., Hoffmeister V. H., Nasserri A., Stahl O., Zinnecker H., 2012, *MNRAS*, 424, 1925
- Dalcanton J. J. et al., 2012, *ApJ*, 200, 18
- Davidson K., 1987, *ApJ*, 317, 760
- Davidson K., Humphreys R. M., 1997, *ARA&A*, 35, 1
- Dessart L., Livne E., Waldman R., 2010, *MNRAS*, 405, 2113
- Dolphin A. E., 2000, *PASP*, 112, 1383
- Draine B. T., 2011, *Physics of the Interstellar and Inter-galactic Medium*
- Draine B. T., Lee H. M., 1984, *ApJ*, 285, 89
- Elitzur M., Ivezić Ž., 2001, *MNRAS*, 327, 403
- Foellmi C. et al., 2008, *Rev. Mexicana Astron. Astrofis.*, 44, 3
- Freedman W. L. et al., 2001, *ApJ*, 553, 47
- Gerke J. R., Kochanek C. S., Stanek K. Z., 2014, *arXiv:1411.1761*
- Horiuchi S., Beacom J. F., Kochanek C. S., Prieto J. L., Stanek K. Z., Thompson T. A., 2011, *ApJ*, 738, 154
- Humphreys R. M., Davidson K., 1994, *PASP*, 106, 1025
- Humphreys R. M., Davidson K., Smith N., 1999, *PASP*, 111, 1124
- Ivezic Z., Elitzur M., 1997, *MNRAS*, 287, 799
- Ivezic Z., Nenkova M., Elitzur M., 1999, *astro-ph/9910475*
- Khan R., Kochanek C. S., Stanek K. Z., Gerke J., 2014, *arXiv:1407.7530*
- Khan R., Stanek K. Z., Kochanek C. S., 2013, *ApJ*, 767, 52
- Kochanek C. S., 2009, *ApJ*, 707, 1578
- Kochanek C. S., 2011a, *ApJ*, 741, 37
- Kochanek C. S., 2011b, *ApJ*, 743, 73
- Kochanek C. S., 2014a, *arXiv:1407.5622*
- Kochanek C. S., 2014b, *MNRAS*, 444, 2043
- Kochanek C. S., 2014c, *arXiv:1407.7856*
- Kochanek C. S., 2014d, *ApJ*, 785, 28
- Kochanek C. S., Beacom J. F., Kistler M. D., Prieto J. L., Stanek K. Z., Thompson T. A., Yüksel H., 2008, *ApJ*, 684, 1336
- Kochanek C. S., Szczygiel D. M., Stanek K. Z., 2011, *ApJ*, 737, 76
- Kochanek C. S., Szczygiel D. M., Stanek K. Z., 2012, *ApJ*, 758, 142
- Krist J., 1995, in *Astronomical Society of the Pacific Conference Series*, Vol. 77, *Astronomical Data Analysis Software and Systems IV*, Shaw R. A., Payne H. E., Hayes J. J. E., eds., p. 349
- Krist J. E., Hook R. N., Stoehr F., 2011, in *Society of Photo-Optical Instrumentation Engineers (SPIE) Conference Series*, Vol. 8127, *Society of Photo-Optical Instrumentation Engineers (SPIE) Conference Series*
- Kushnir D., Katz B., 2014, *arXiv:1412.1096*
- Lamers H. J. G. L. M., de Groot M., Cassatella A., 1983, *A&A*, 123, L8
- Li W., Filippenko A. V., Van Dyk S. D., Hu J., Qiu Y., Modjaz M., Leonard D. C., 2002, *PASP*, 114, 403
- Mathis J. S., Rumpl W., Nordsieck K. H., 1977, *ApJ*, 217, 425
- Pan K.-C., Ricker P. M., Taam R. E., 2013, *ApJ*, 773, 49
- Pastorello A. et al., 2004, *MNRAS*, 347, 74
- Pejcha O., Thompson T. A., 2014, *arXiv:1409.0540*
- Prieto J. L. et al., 2008, *ApJ*, 681, L9
- Puls J., Vink J. S., Najarro F., 2008, *A&A Rev.*, 16, 209
- Saha A., Sandage A., Tammann G. A., Labhardt L., Macchetto F. D., Panagia N., 1999, *ApJ*, 522, 802
- Schlafly E. F., Finkbeiner D. P., 2011, *ApJ*, 737, 103
- Schlegel D. J., Finkbeiner D. P., Davis M., 1998, *ApJ*, 500, 525
- Shappee B. J., Kochanek C. S., Stanek K. Z., 2013, *ApJ*, 765, 150
- Smartt S. J., 2009, *ARA&A*, 47, 63
- Smith N., Humphreys R. M., Gehrz R. D., 2001, *PASP*, 113, 692
- Smith N., Li W., Silverman J. M., Ganeshalingam M., Filippenko A. V., 2011, *MNRAS*, 415, 773
- Smith N., Owocki S. P., 2006, *ApJ*, 645, L45
- Spiro S. et al., 2014, *MNRAS*, 439, 2873
- Thompson T. A., Prieto J. L., Stanek K. Z., Kistler M. D., Beacom J. F., Kochanek C. S., 2009, *ApJ*, 705, 1364
- Treffers R. R., Peng C. Y., Filippenko A. V., Richmond M. W., Barth A. J., Gilbert A. M., 1997, *IAU Circ.*, 6627, 1
- Turatto M. et al., 1998, *ApJ*, 498, L129
- Ugliko M., Janka H.-T., Marek A., Arcones A., 2012, *ApJ*, 757, 69
- Van Dyk S. D., Filippenko A. V., Chornock R., Li W., Challis P. M., 2005, *PASP*, 117, 553
- Van Dyk S. D., Matheson T., 2012, in *Astrophysics and Space Science Library*, Vol. 384, *Astrophysics and Space Science Library*, Davidson K., Humphreys R. M., eds., p. 249
- Van Dyk S. D., Peng C. Y., Barth A. J., Filippenko A. V., 1999, *AJ*, 118, 2331
- Van Dyk S. D., Peng C. Y., King J. Y., Filippenko A. V., Treffers R. R., Li W., Richmond M. W., 2000, *PASP*, 112, 1532
- Wagner R. M. et al., 2004, *PASP*, 116, 326
- Weis K., Bomans D. J., 2005, *A&A*, 429, L13
- Woosley S. E., Heger A., 2015, in *Astrophysics and Space Science Library*, Vol. 412, *Astrophysics and Space Science Library*, Vink J. S., ed., p. 199
- Woosley S. E., Weaver T. A., 1995, *ApJS*, 101, 181